



Flood Susceptibility Assessment Using Frequency Ratio Model: A Case Study of District Ghotki and District Kashmore, Sindh, Pakistan

Awais Munir¹, Muhammad Bachal Alias Sahib Khan², Muhammad Asad Ghufra³,
Noor Fatima⁴

¹ PhD Scholar at Department of Environmental Science, International Islamic University Islamabad, Pakistan. Lecturer at Institute of Agro-Industry and Environment, Faculty of Agriculture and Environment, The Islamia University of Bahawalpur, Pakistan. Email: awais.munir@iub.edu.pk

² MS Scholar at Institute of Agro-Industry and Environment, Faculty of Agriculture and Environment, The Islamia University of Bahawalpur, Pakistan. Email: mbachalkhan@gmail.com

³ Professor at Department of Environmental Science, International Islamic University Islamabad, Pakistan. Email: asad.ghufra@iiu.edu.pk

⁴ PhD Scholar at Centre of Excellence in Water Resource Engineering, University of Engineering and Technology, Lahore, Pakistan. Email: noorfatima0437@gmail.com

ARTICLE INFO

Article History:

Received: February 11, 2025
Revised: April 27, 2025
Accepted: May 04, 2025
Available Online: May 06, 2025

Keywords:

Climate Change
Economy
Environment
Flood
Pakistan

JEL Classification Codes:

Q54, O5, Q56, Q25, R14

Funding:

This research received no specific grant from any funding agency in the public, commercial, or not-for-profit sectors.

ABSTRACT

In recent years, flash floods in Ghotki and Kashmore districts in Pakistan have seriously affected both people and their ways of earning a living. Addressing challenges related to flooding means utilizing a methodology that considers both the hydrology, of water, the environment, the soil, the economy and social impacts. Flood susceptibility mapping helps inform how to control and plan floods. A bivariate probability analysis employing the frequency ratio (FR) methodology was conducted during this investigation to develop flood vulnerability assessments for Ghotki and Kashmore. A map was produced using the 130 past flood locations in the two districts. To establish the models, the data from these localities were randomly divided into 70% for model development and 30% for assessment. Among the parameters incorporated in the analysis were aspect, slope, elevation, rainfall, type of soil, use of land, proximity to roadways and rivers and NDVI and NDSI figures. How each factor affects flooding was assessed by checking its relationship with previous floods. From the analysis, scientists found that approximately 18% of the study area was classified as extremely flood susceptible, 30.9% as highly flood susceptible, 20.7% as moderately flood susceptible, 20.6% as minimal flood susceptibility and 9.8% as negligible flood susceptibility. Using the metrics from the validation set, the Foul Reader showed an accurate prediction rate of 75%. Moreover, the resulting susceptibility maps were compared to the real floods of 2010 and 2022, showing that the model reliably predicts flood-prone areas. As a result, the FR model is demonstrated to support the activities of governmental organizations, administrators and policy-makers in preventing and managing floods in the region.



© 2025 The Authors, Published by iRASD. This is an Open Access Article under the [Creative Common Attribution Non-Commercial 4.0](https://creativecommons.org/licenses/by-nc/4.0/)

Corresponding Author's Email: awais.munir@iub.edu.pk

Citation: Munir, A., Khan, M. B. A. S., Ghufra, M. A., & Fatima, N. (2025). Flood Susceptibility Assessment Using Frequency Ratio Model: A Case Study of District Ghotki and District Kashmore, Sindh, Pakistan. *iRASD Journal of Energy & Environment*, 6(1), 31–46. <https://doi.org/10.52131/jee.2025.0601.0053>

1. Introduction

Floods are considered one of the deadliest natural hazards for people everywhere (Mehravara et al., 2023). They harm many people, result in a lot of building damage, lead to economic losses and spark lots of uneasiness in society (Mitra & Das, 2022). As a result of climate change and the effects of fast urban growth and poor land use, floods in many countries have been more damaging lately (Choudhury et al., 2022). Due to the many economic and social effects it causes, experts from many places are studying this issue (Das, 2020). UNISDR data shows that during the years 1995 to 2015, there were nearly 150,061 global flood incidents causing 157,000 deaths because of floods. Eleven percent of all the fatalities from disasters worldwide occurred during such incidences (Wang et al., 2018). Many researchers claim that an average of 200 million people each year are affected by floods (Bui et al., 2019). Also, estimates based on climate change, changes in land use and a growing population mean there could be greater flooding by 2050, causing damages worth around US\$ 1 trillion (Alexander et al., 2019).

Floods may be categorized by four types: flash floods, riverine floods, coastal floods and urban floods (Costache & Tien Bui, 2020). When compared to other floods, flash floods bring the highest risk because they can take both many lives and cause extensive property damage very quickly (Bui et al., 2019). In addition, the river region carries a great deal of sediment which damages equipment and claims the lives of many people (Islam et al., 2021). Both developing and developed countries have experienced very serious flood damage (Mashaly & Ghoneim, 2018). In comparison to developed countries, developing nations are more at risk for flash floods owing to a lack of appropriate infrastructure, enough resources and the needed technology to predict flooding. Consequently, there exists a critical imperative to establish sophisticated prediction models for assessing flood event probability and to conduct susceptibility mapping of inundation-prone regions (Buba et al., 2021).

Pakistan has a history marked by devastating floods. The 2010 flood alone resulted in losses amounting to ten billion USD. Based on thirty years of disaster data, floods have been consistently reported in Pakistan (Munir et al., 2022). The 2022 monsoon floods had severe consequences in Sindh, including its northern regions, where approximately one-third of Pakistan was submerged. Monsoon rains triggered widespread flooding, particularly affecting the provinces of Sindh and Balochistan. Pakistan had never previously encountered an uninterrupted cycle of monsoon torrents lasting eight consecutive weeks, resulting in extensive inundation across the country (Qamer et al., 2022). The relentless torrents led to long-term displacement for approximately 7.9 million people. Many individuals lost their homes and livelihoods, exacerbating enduring humanitarian needs. Over 4.4 million acres of agricultural land were destroyed, significantly impacting the livelihoods of farmers and exacerbating food insecurity in the region.

Ghotki and Kashmore districts in the north of Sindh saw a great deal of damage to their infrastructure, a significant loss of farm crops and significant problems for local people. Because of destroyed roads and bridges, flooded land and ruined embankments, thousands in the region faced long-term challenges to their wellbeing and their economic prospects. Northern Sindh's roads, bridges and irrigation systems were badly damaged as protective walls broke down and many towns and villages were flooded. As a result, floods caused great harm to both public and personal property. It is important to take steps to control and prevent floods to save natural resources, fields, infrastructure and other important assets (Qamer et al., 2022). For this reason, understanding the risk of flooding is crucial for both forecasting and emergency services, since this knowledge supports improvement of management methods against future flooding (Tehrany et al., 2015).

In many parts of the world, researchers depend on MCDA, RS and GIS techniques to reliably analyze and mark flood-prone regions. This approach becomes especially useful in areas where enough data is missing, allowing local planners to use it for flood control (Zou et al., 2013). Wang et al. (2018) observed that the AHP method has uncertainty because it depends on input from experts. The Food Risk (FR) model is valued because it is

straightforward and creates detailed food risk analysis and maps that many can understand and use (Liao & Carin, 2009). Although fairly new in the field of flood modeling, an FR model has become common in studies of landslides (Munir et al., 2022). Flood susceptibility maps made using the FR model should be used in plans aimed at lowering flood risks and their consequences, according to studies (Lee et al., 2012).

Simulating floods is a challenging job because many considerations are needed. Flood mapping and risk assessment rely greatly on Remote Sensing (RS) technology which is very important for these tasks. RS, in combination with GIS, helps quickly collect, store, organize, work with, find, interpret and present information needed for finding hazard areas. In this work, we use multiple methods to show that flood modeling works well when brought together with geographic information systems. Both RS and GIS techniques were added to the Frequency Ratio (FR) approach for estimating flooding probabilities. The research looks at how Geographic Information Systems, Remote Sensing and Frequency Ratio models are used to assess and predict the chance of floods in Ghotki and Kashmore Districts. The main goal is to find and exactly define the flood susceptibility areas in the districts. The objective is to make flood susceptibility maps for Ghotki and Kashmore, conduct impact studies and gather substantial data for the FR model to categorize likely flood zones. The information helps people responsible for local government create ways to handle flooding.

2. Materials and Methodology

2.1. Study Area

The region of District Ghotki in Sindh, Pakistan is situated between latitudes 28°24'N to 28°55'N and longitudes 69°07'E to 69°43'E. Current data suggests the population approximates 1.6 million. Ghotki is located adjacent to Kashmore territory toward the northern boundary, India toward the southern boundary, Sukkur territory toward the eastern border and Rahim Yar Khan district in Punjab province to the northeast. Within this district, summer thermal conditions routinely surpass 40°C (104°F), while winters remain comparatively moderate with average thermal readings ranging between 10°C and 25°C (50°F to 77°F). Precipitation predominantly occurs throughout the monsoon period which extends from July through September, rendering the territory notably arid. Located in northern Sindh, Pakistan, District Kashmore is encompassed by longitudes from 69°16'E to 70°15'E and latitudes from 28°08'N to 28°54'N. Approximately 1.2 million inhabitants reside in Kashmore which shares boundaries with Jacobabad territory toward the western edge, Ghotki territory toward the southern perimeter and Punjab province to the northeast. The district's climatic conditions are characteristic of the region, featuring extended scorching summers exceeding 45°C (113°F) and temperate winters with thermal measurements ranging from "10°C to 25°C (50°F to 77°F)."

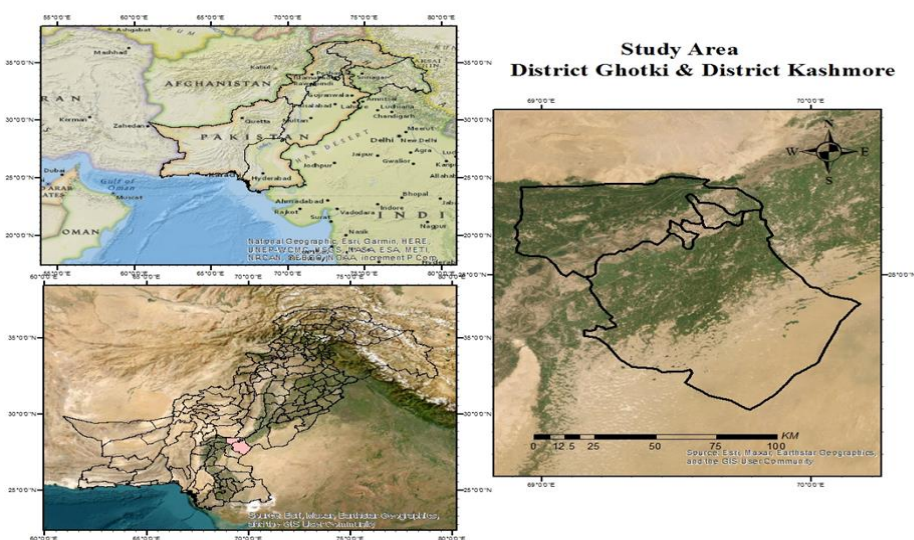


Figure 1: Location Map of the Study Area

2.2. Methodology

The purpose of creating a flow chart was to explain all the stages in the project: reviewing the flood inventory map, developing variables that depend on flood conditions, ranking those variables using the Initial, multi-collinearity test and information gain ratio the frequency ratio is applied to the current investigation (Table 1).

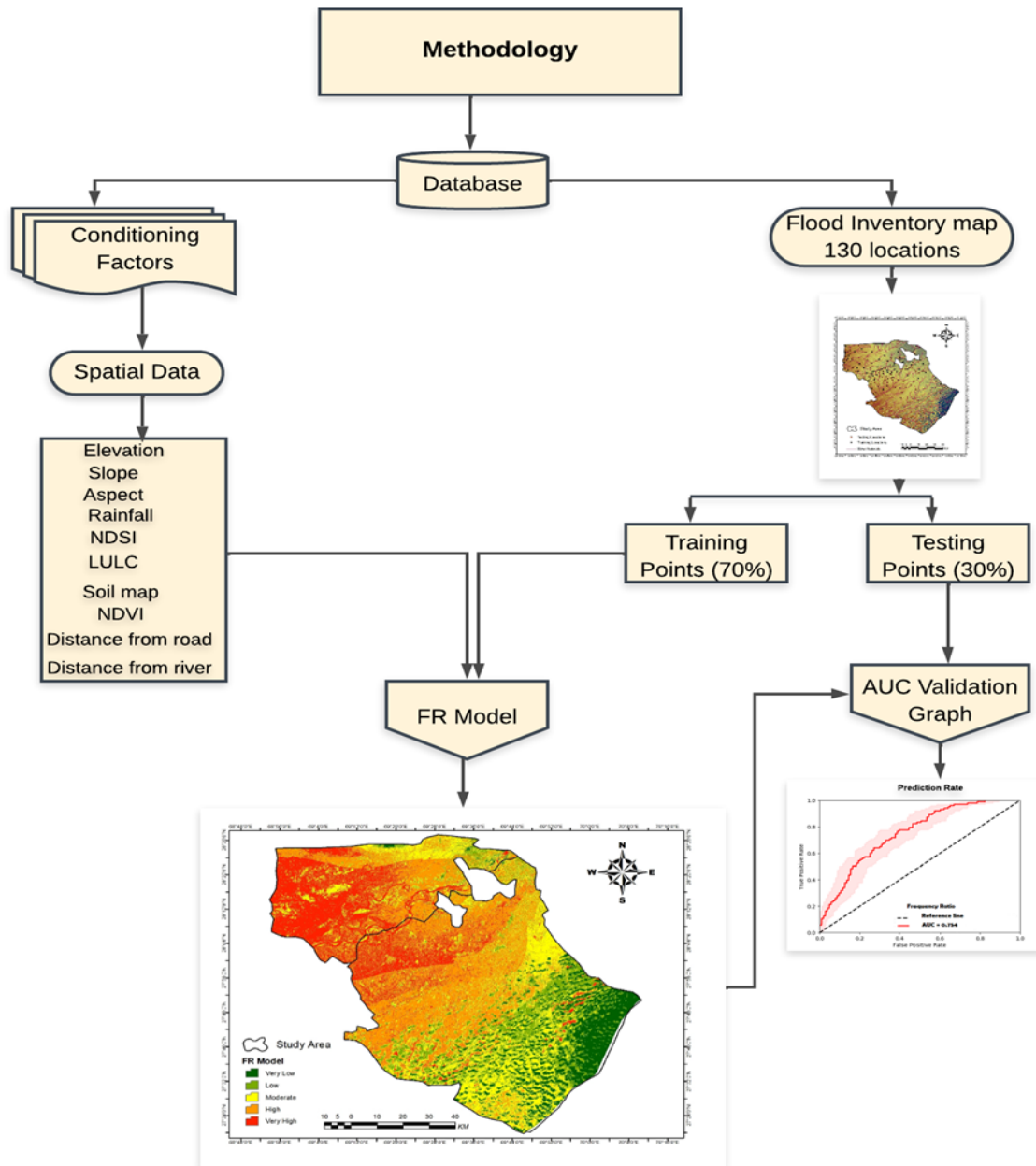


Figure 2: Showing Research Methodology of the Study Area

2.3. Flood Inventory Map

Food inventory (FI) data is the historical record of flood-prone locations and is often generated using historical records. The FI map is excellent for forecasting future floods (Rahmati et al., 2016). For the inventory, 130 flood-prone locations were selected. Random points were employed in the study because the algorithm and results amplification are difficult when using the polygon layout of the catalog. Most associated natural hazard modeling has used this format for inventory data. (Paradhan et al., 2010). The entire dataset was divided into a 70/30 ratio, in which 91 points (70%) of the dataset were selected randomly to run the model, and 39 points (30%) were used for in validation (Fig 2).

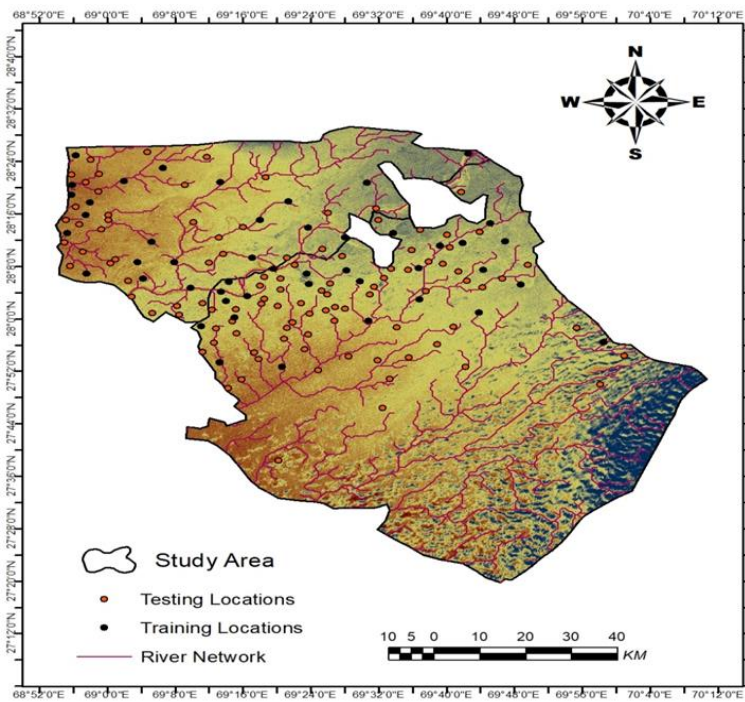


Figure 3: Inventory Map of the Research Area

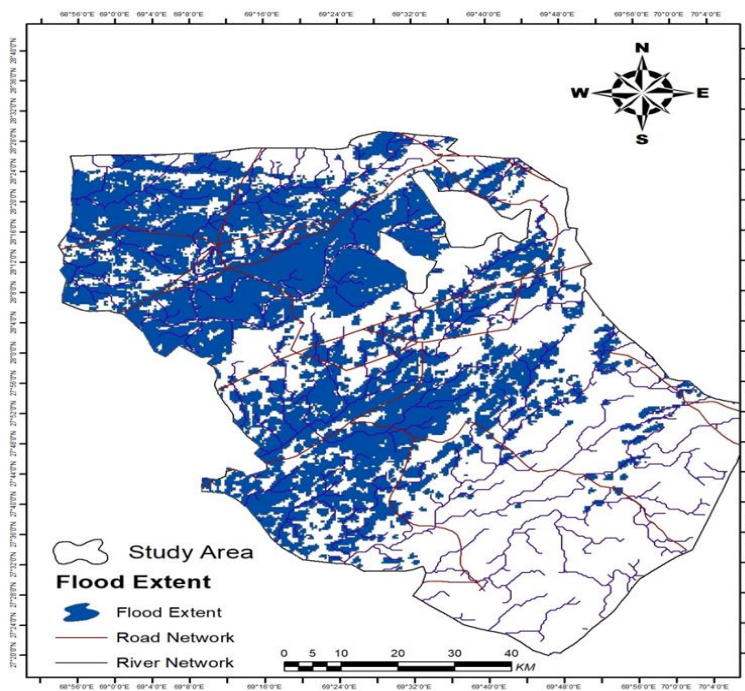


Figure 4: Flood Extent in the Study Area During 2022

2.4. Preparing Flood Conditioning Factors

Establishing a solid spatial flood susceptibility model is difficult because it takes extensive data on the land, earth and water systems. Picking out the main factors that drive floods is crucial, since it helps us check if flood susceptibility maps are accurate. The nine factors used to describe flood conditioning in this research area are elevation, slope, aspect, land use/land cover (LULC), distance from the road, distance from the river, soil type and rainfall, each based on the accessible literature on flood vulnerability. Using NDSI and NDVI, after being recommended by Sturzenegger et al. (2019). All the data was processed to a 30-meter-spatial resolution raster format. Flood modeling results depend on changes in underlying landscapes, so they are highly significant (Lu et al., 2020). An early ArcGIS 10.8

version was used to make a DEM map for the study area, sourcing the ASTER GDEM (version 2) at a resolution of 30 meters. All slope, aspect, distance to highways and distance to rivers were obtained using the DEM. Such aspects affect future efforts in modeling and studying floods.

Elevation is a main piece in the puzzle when considering flood modeling. It also means floodwater follows the slope and reaches further or stays closer as needed (Dodangeh et al., 2020). You're more unlikely to see flooding at higher altitudes because rain or snow collected on ascending terrain moves in a slower and less concentrated way. Flooding is more likely in low-lying locations, because water flows naturally downwards (Wang et al., 2018). Their location along the Indus River and their flat landscape mean the areas flood much more frequently. The low terrain and site close to a large river make areas around it more at risk from flooding after strong rain or increased river discharge. The slope determines the rate of water flow and is very important in causing floods, as reported by Stevaux et al. in 2020. To put it simply, a higher slope angle means water is more likely to flow, will infiltrate less and the water will move at greater speed. As a result, places that are level and not high such as the Ghotki and Kashmore districts, are more likely to be affected by flooding (Fig. 4b). In addition, one feature shapes the direction of floodwater and helps protect soil moisture (Chen et al., 2020). In this way, flooding is influenced by the factor as well. Areas with high moisture in the soil are one cause of sudden and heavy runoff (Fig. 4c).

Floods occur more frequently when surface runoff and sediment transportation are increased because of changes in land use and land cover (Siswanto & Francés, 2019). The type of land use controls the generation and flow of surface runoff. Since water cannot sink into built-up areas, their surface levels rise more quickly and floods happen more often. No water seepage takes place in dense forests and thus flooding is often avoided there (Abd El-Hamid et al., 2021). At all timescales, the reaction of water to floods is negatively linked to the quantity of vegetation (Dodangeh et al., 2020). For the study, we processed Sentinel-1 satellite images to generate the Land Use Land Cover (LULC) map at a scale of 30 meters per pixel. We chose supervised algorithms in ERDAS to carry out LULC classification. For the LULC map, classes were designed as vegetation, water, desert area, bare land and built-up area (Fig. 4g). Because most sites hit by floods are beside rivers, localization of the model in relation to rivers plays a vital role. According to Tehrany et al. (2015) the distance from the stream is a major factor in identifying places at risk of flooding in a basin (2015). A location close to the river can experience severe flooding, as river flow more easily affects it (Gupta, 2020).

Floods have a lower chance of occurring the further you go away from the river. The volume of water held in the soil at the basin level controls the size of water-related flooding in specific regions (Van Binh et al., 2020). In the present work, the Euclidean Distance tool within the Spatial Analyst toolset in ArcMap 10.4 was applied to make the distance-from-rivers layer (Fig 4h). The farther a location is from roads, the greater the surface water runoff and difficulty with draining water which makes those locations more likely to be affected by floods. It is important to grasp this idea for successful flood risk assessment, prevention and the design of cities. In ArcMap 10.8, the Euclidean Distance tool from the Spatial Analyst toolbox was implemented to prepare the distance-from-rivers layer (Fig. 4i). How soil is formed affects the way in which rainwater is drained (Zhao et al., 2019). How soil properties affect water absorption affects the generation of runoff. Nevertheless, nearby conditions such as the local weather and the way soil is eroded can have a big effect on rainfall-runoff. A higher rate of infiltration is linked to lower numbers of flooding (Philip et al., 2019).

A soil map was created in this study using the FAO soil portal and this was then assigned to three classes (Fig. 4j). It has been discovered that rainfall greatly affects flooding incidents (Pourghasemi et al., 2021). Floods often happen because of a sudden intense downpour (Peptenatu et al., 2020). Rainfall information used in the study was taken from the Pakistan Meteorological Department database and rainfall maps were constructed with ArcGIS 10.8 using the kriging interpolation method (see Fig. 4e). NDSI was computed and acquired from a range of Sentinel-1 bands. Analytical methods displayed in NDSI (Fig. 4d) may be

used to gather improved data on soil properties from both vegetation and impermeable surfaces. By using the ratio between blue and red wavelengths in the ArcGIS Raster calculator, researchers could recognize areas of exposed soil, as well as other coverage types, including vegetation (Regmi et al., 2014). Using the (Eq.1), NDSI can be computed.

$$NDSI = \frac{Band3 - Band11}{Band3 + Band11} \quad (1)$$

The relationship between vegetation and these bands was measured using the Normalized Difference Vegetation Index (NDVI). A high number on the ecotope scale is a sign that a location is a rainforest and a low number tells you it is a barren place like rock, sand or snow (Munir et al., 2022). Numerous free images from the Sentinel-1 satellite were found using the USGS Earth Explorer which is found at this link: <https://earthexplorer.usgs.gov/> It is shown here with Equation 2:

$$NDVI = \frac{Band5 - Band7}{Band5 + Band4} \quad (2)$$

Table 1
Data Source of Research

S. No	Primary Data	Spatial Resolution	Format	Source of Data
1	SRTM (DEM)	30m	Raster	https://opentopography.org/
2	Sentinel-2	10 m	Raster	https://earthexplorer.usgs.gov
3	Soil Data	1:100,000	Vector	https://www.fao.org/soils-portal/data-hub/soil-maps-and-databases/en/
4	Rainfall Data	1:100,000	Raster	https://www.pmd.gov.pk/en/

2.5. Bivariate Statistical Analysis (BSA)

2.5.1. Frequency Ratio Model (FR)

Analysis of frequency ratios (FR) is a prominent bivariate technique extensively employed in flood susceptibility studies. It assesses the geographical association between independent and dependent variables. The choice of training locations considered the geography, climate and characteristics of each area, all considered individually in the analysis. The research successfully used the frequency ratio model to study flood susceptibility in numerous regions around the world (Khosravi et al., 2016).

$$FR = \frac{\text{Flood Points in Factor} \div \text{Total Flood Points}}{\text{Flood Class Area} \div \text{Total Area}} \quad (3)$$

After working out the FR values for each class, all the data for each contributing factor was merged to produce the final flood susceptibility map. To make a map for contributing areas that flood, the RF was calculated inside of the same probability range ([0, 1]) using Equation 4.

$$RF = \frac{\text{Factor class FR}}{\sum \text{Factor class FR}} \quad (4)$$

After normalization, every aspect it looks at is given the same weight which is another drawback of RF. Each source of floods was estimated using Equation 5, with the prediction rate (PR) or weight fine-tuned to deal with this issue and form mutual links among them.

$$PR = (RF_{max} - RF_{min}) / (RF_{max} - RF_{min}) \quad (5)$$

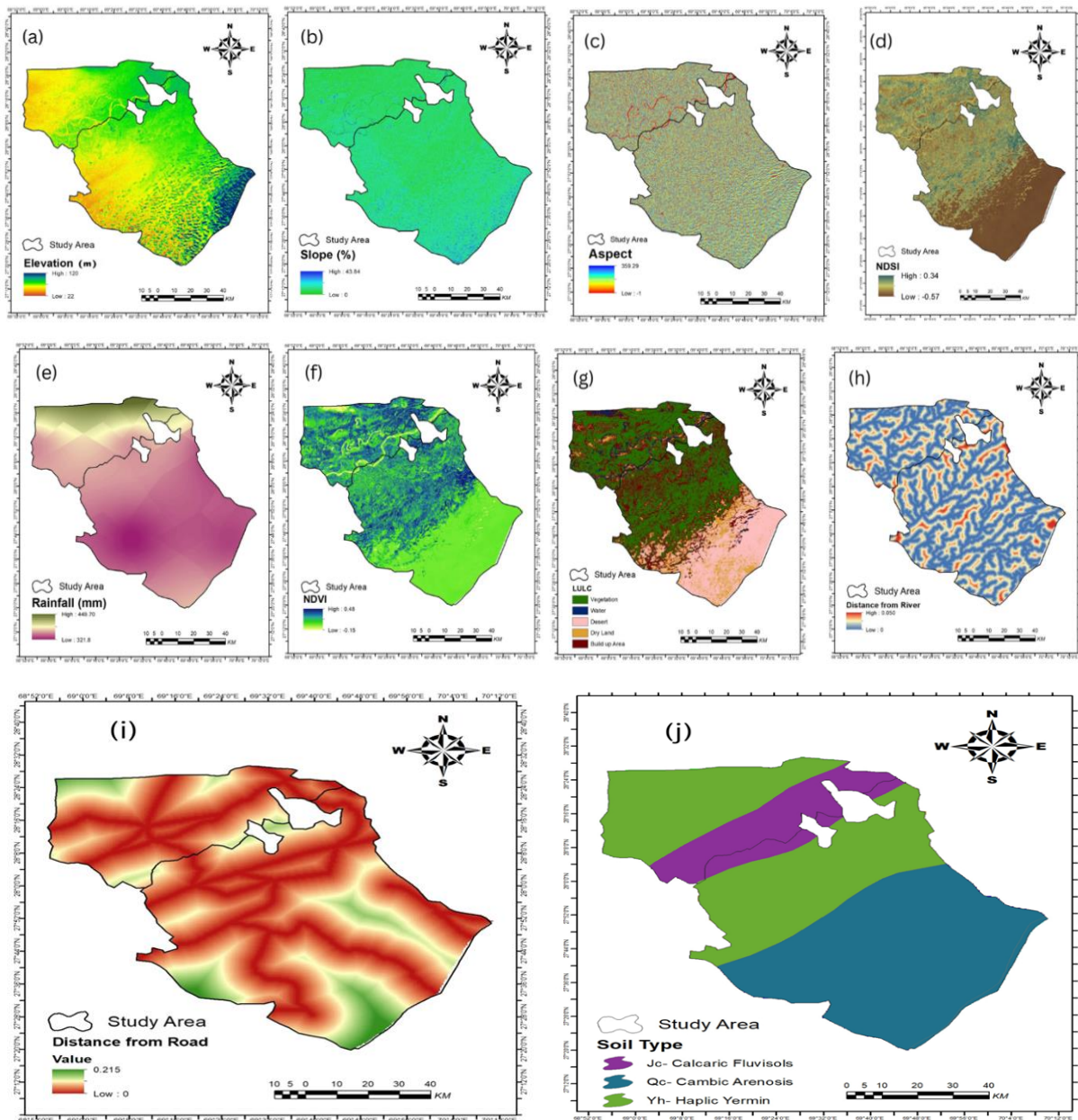


Figure 5: Parameters Used for FR Modeling (a) Elevation (b) Slope (c) Aspect (d) NDSI (e) Rainfall (f) NDVI (g) LULC (h) Distance from River (i) Distance from Road (j) Soil Type

**Table 3
Results of the Frequency Ratio Analysis (FR) of Each Factor**

Parameters	Class	Class Pixels	% Class Pixels	Flood Pixels	% Flood Pixels	FR	RF
Slope	< 1.37	4518555	45.0	2124962	51.1	0.470	0.276
	1.37 - 2.75	3390231	33.8	1378732	33.1	0.407	0.239
	2.75 - 4.47	1548214	15.4	506089	12.2	0.327	0.192
	4.47 - 7.39	504786	5.0	133359	3.2	0.264	0.155
	7.39 - 43.84	77556	0.8	18388	0.4	0.237	0.139
Elevation	< 65	1876875	18.7	1034830	24.9	0.551	0.359
	65-70	3600391	35.8	1769468	42.5	0.491	0.320
	70-76	3359262	33.4	1248235	30.0	0.372	0.242
	76-86	959421	9.5	110694	2.7	0.115	0.075
	86-120	260328	2.6	1018	0.0	0.004	0.003
LULC	Vegetation	832421	8.3	457753	11.0	0.550	0.262
	Water	1428796	14.2	906430	21.8	0.634	0.302

	Desert	3417103	34.0	1849696	44.4	0.541	0.258
	Bare land	3201740	31.8	807692	19.4	0.252	0.120
Aspect	Built up	1176279	11.7	142578	3.4	0.121	0.058
	< 63.99	1900159	18.9	852675	20.5	0.449	0.216
	63.99- 140.29	1890276	18.8	753814	18.1	0.399	0.192
	140.29- 212.34	2208269	22.0	898622	21.6	0.407	0.196
	212.34 - 282.99	2059220	20.5	844216	20.3	0.410	0.198
Rainfall	282.99 - 359.29	1981418	19.7	812203	19.5	0.410	0.198
	< 344	4511148	47.0	1406140	35.1	0.312	0.152
	344 - 362	3572230	37.3	1608271	40.2	0.450	0.219
	362 - 384	879575	9.2	622617	15.6	0.708	0.345
	384 - 409	626355	6.5	365657	9.1	0.584	0.284
NDVI	409 - 449	467067	4.9	162272	4.1	0.347	0.169
	< 0.007	255693	2.6	181769	4.4	0.711	0.275
	0.007- 0.10	4115573	41.1	845500	20.3	0.205	0.079
	0.10- 0.20	1990598	19.9	1192477	28.6	0.599	0.232
	0.20 - 0.30	1714830	17.1	999163	24.0	0.583	0.225
Soil map	0.30 - 0.48	1940273	19.4	945218	22.7	0.487	0.188
	Sandy Loam	1353329	23.7	1031060	24.8	0.762	0.069
	Loam	1781313	31.1	1125668	27.1	0.632	0.057
	Sandy Clay loam	2493196	43.6	1141682	27.4	0.458	0.041
	Clay loam	93631	1.6	862535	20.7	9.212	0.833
NDSI	< -0.197	39	0.0	18	0.0	0.462	0.246
	-0.19 - -0.013	3735874	37.3	552075	13.3	0.148	0.079
	-0.013 - 0.07	2251047	22.5	1375849	33.0	0.611	0.326
	0.07 - 0.17	1870199	18.7	1138666	27.3	0.609	0.325
	0.17 - 0.34	2159808	21.6	1097519	26.4	0.508	0.271
Distance From River	<0.006	3867783	62.9	1802039	76.4	0.466	0.327
	0.006 - 0.014	3115021	50.7	1243239	52.7	0.399	0.280
	0.014 - 0.020	1612078	26.2	618167	26.2	0.383	0.269
	0.020- 0.028	1208641	19.7	437093	18.5	0.362	0.254
	0.028 - 0.050	213982	3.5	60029	2.5	0.281	0.197
Distance From Road	< 0.026	3471817	23.7	1464423	54.3	0.422	0.294
	0.026 - 0.056	2678973	7.7	1233386	45.7	0.460	0.321
	0.056 - 0.088	2106544	1.2	906368	33.6	0.430	0.300
	0.088 - 0.129	1278804	28.7	474192	17.6	0.371	0.259
	0.129 - 0.215	482020	55.0	83289	3.1	0.173	0.120

You get the flood vulnerability index by adding each PR to the RF for each class, according to Equation 6.

$$FVI = \sum_{j=1}^n FR \tag{6}$$

2.6. Model Validation

Ghotki and Kashmore Districts were marked on the flood susceptibility map following confirmation from using the Area Under the Curve (AUC) procedure. This approach, backed by science, reviews the FR model by examining the results with historic floods. Frequently referred to as the best method for testing FR models, the AUC method has seen use in several important research studies (Rahman et al., 2021).

$$AUC = \sum_{i=1}^{n=100} \frac{(X1+X2)}{2(Y2+Y1)} \tag{7}$$

Ranges of accuracy levels are: 0.50–0.60 as having low accuracy, 0.61–0.70 modest accuracy, 0.71–0.80 excellent accuracy, 0.81–0.90 very good accuracy and 0.91–1.00 outstanding accuracy (Yesilnacar & Hunter, 2004).

3. Results and Discussion

The flood susceptibility of Ghotki and Kashmore districts was estimated using elevation, land use/cover (LULC), normalized difference soil index (NDSI), slope, aspect,

curvature, rainfall, NDVI, distances from rivers and roadways and soil type. These factors were systematically evaluated to quantify the region's vulnerability to flooding events.

The study area exhibits a range of elevations, with the highest point recorded at 120 meters and the lowest at 22 meters. Maximum elevations are concentrated in the southeastern desert region along the Indian border and small pockets in the southwestern part of the area (Fig. 4a). Slope angles, derived from DEM data, were categorized into five classes: $< 1.3^\circ$, $1.3\text{--}2.7^\circ$, $2.7\text{--}4.4^\circ$, $4.4\text{--}7.3^\circ$, and $> 7.3^\circ$. Areas with flatter slopes ($< 1.3^\circ$) are predominantly located on both sides of the study area, marked in green (Fig. 4b). Lower slope gradients are associated with increased vulnerability to floods and flood-related incidents (Rahmati et al., 2016). Higher Flood Ratio (FR) values were observed in two lower slope gradient classes: $< 1.3^\circ$ with an FR of 0.47 and $1.3\text{--}2.7^\circ$ with an FR of 0.4. In contrast, the area with a slope of 7.3° exhibited a lower FR value of 0.23 (Table 3). Aspect plays a significant role in hydrological processes, influencing evapotranspiration, frontal precipitation patterns, weathering, and the establishment of vegetation, especially in desert regions (Pourghasemi et al., 2013). In the study area, specific aspect ranges, such as < 63.99 , 212.34 to 282.99 , and 282.99 to 359.29 , exhibited high Flood Ratio (FR) values of 0.216 and 0.198, respectively (Table 3).

Rainfall distribution across the study area was categorized into five classes (< 344 , $344\text{--}362$, $362\text{--}384$, $384\text{--}409$, and > 409 mm) using ArcGIS 10.8 software. The northern side of the Kashmore district recorded the highest rainfall, while the extreme southwest desert area of the Ghotki district received the lowest precipitation (Fig. 4e). Analysis revealed that rainfall ranges between 362 to 384 mm and 384 to 409 mm exhibited high Flood Ratio (FR) values of 0.70 and 0.58, respectively, indicating increased flood susceptibility in these areas (Table 3). The study area's land cover and land usage were divided into five categories: vegetation, water, desert, dryland, and built-up. Following classification, the results indicate that 43% of the area is covered by vegetation, 2% by water, 20% by desert in the southeastern part, 20% by dryland, and 24% by built-up areas (Fig. 4g). In terms of flood susceptibility, water, and vegetation classes exhibited high Flood Ratio (FR) values of 0.63 and 0.55, respectively, suggesting elevated vulnerability to flooding in these land cover types (Table 3).

Flood susceptibility is significantly influenced by the Normalized Difference Vegetation Index (NDVI) assessment, with values ranging from -1 to $+1$ (Khosravi et al., 2016). According to Khosravi, negative NDVI values indicate water presence, while positive values signify vegetation cover, establishing a negative association between NDVI and flood risk (Paul et al., 2019). While lower NDVI levels indicate a higher danger of flooding, higher NDVI values indicate a higher susceptibility to flooding. In the study area, NDVI ranges < 0.007 and 0.10 to 0.20 exhibited high Flood Ratio (FR) values of 0.711 and 0.599, respectively, highlighting areas with increased flood susceptibility (Table 3). Using the Normalized Difference Soil Index (NDSI), differences in the study area's soil composition using satellite imagery. Deng developed the Modified Normalized Difference Water Index (MNDWI), which depends on bare soil's high reflectance in the shortwave infrared wavelength and is inverted to create the NDSI. Despite its capability to identify large, dry bare soil areas, it may overlook smaller, scattered patches. Thermal infrared wavelength (TIR) was utilized for bare land detection (Aghdam et al., 2016).

Results indicated that NDSI values ranging from -0.19 to -0.007 and 0.07 to 0.17 exhibited high Flood Ratio (FR) values of 0.61 and 0.60, respectively, indicating areas with increased flood susceptibility in the study area (Table 3). Distance from roads significantly influences flood susceptibility and vulnerability mapping. Impervious roads and nearby urban surfaces play a crucial role in determining flood levels by limiting terrain permeability and serving as runoff outlets (Shuster et al., 2005). In the study area, maximum Flood Ratio (FR) values of 0.46 and 0.43 were observed, corresponding to distance class levels of 0.026 to 0.056 and 0.056 to 0.088 , respectively (Table 3). These findings underscore the impact of road infrastructure on flood dynamics and vulnerability assessment in the region. The distance from the river is an important consideration when determining flood risk, as areas

nearest to riverbanks are most susceptible to high water levels following floods. Typically, flood depth is highest near the river mouth or confluence. Regions located farther from these points are categorized as lower risk, whereas those nearby are deemed higher risk (Chapi et al., 2017).

In this study, Less than 0.006 and 0.006 to 0.014 distances from the river showed high Flood Ratio (FR) values of 0.46 and 0.39, respectively (Table 3). These findings emphasize the significant role of river proximity in flood susceptibility mapping and risk assessment. The study area's soils were classified into Calcaric Fluvisols, Cambic Arenosis, and Haplic Yermis. Cambic Arenosis predominates in the southeastern part, while Haplic Yermis is prevalent in the central and western regions. Calcaric Fluvisols are found on both sides of the Indus River, and red gravelly soils cover the extreme northwest (Fig. 4j).

Based on the Frequency Ratio (FR) values derived from each conditioning parameter subclass (as detailed in Table 2), a rating was assigned to assess flood occurrence correlations, ranging from weak (< 1) to strong (> 1) (Lee et al., 2012). The FR model (Eq. 6) indicated that higher FR values corresponded to increased probabilities of flood occurrences. With the use of this model, five flood susceptibility zones were identified for the research area: There are four groups: very low (less than 5.0), low (5.0–7.5), moderate (7.5–10.0), high (10.0–12.5) and very high (more than 12.5) (as shown in Fig. b). Land areas were identified through analysis into various groups determined by flood risk, with 18.3% having a very high risk, 30.9% a high risk, 20.7% a moderate risk, 20.6% a low risk and 9.31% a very low risk (Table 4).

The flood susceptibility changes from part of the study site with moderate to low risk to those facing high or very high levels. This pattern is particularly evident in the central Ghotki district, including the Kacha area, low-lying central district areas, and along the Indus riverside, which are categorized as high-risk to extremely high-risk areas. Additionally, the western part of the Kashmore district is identified as a zone with very high flood risk (Fig. 5). The zones with high to extremely high flood susceptibility are identified by several critical variables that enhance their risk. Examples are land with considerable runoff, sluggishly draining soil, areas with silt and sand sediments, braided floodplains, lands below sea level, weak slope gradients and locations close to the main river. Using the Frequency Ratio approach, these factors are necessary to map which areas in the study area are expected to be most at risk of flooding.

Table 4
Statistical Analysis of Flood Vulnerability Classes in the Study Area

S. No	Flood susceptible class	FR value range	Histogram	% of Area
1	Very low	< 5.0	931794	9.31
2	Low	5.0–7.5	2063310	20.63
3	Moderate	7.5–10.0	2079952	20.79
4	High	10.0–12.5	3092292	30.92
5	Very High	> 12.5	1832947	18.32

Although many models have been designed by researchers to assess flooding, confirming how well they perform is very important. Experiments have shown that the Flood Ratio (FR) model gives accurate results for predictions and forecasting (Chung & Fabbri, 2003). Whenever the accuracy score is 1.0, it means the model can predict natural hazards without showing any preference towards any category (Pradhan & Buchroithner, 2010). This model success rate was assessed by using 39 flood points. It is estimated that possible future flood zones are listed as being of "moderate" or "very high" risk of flooding.

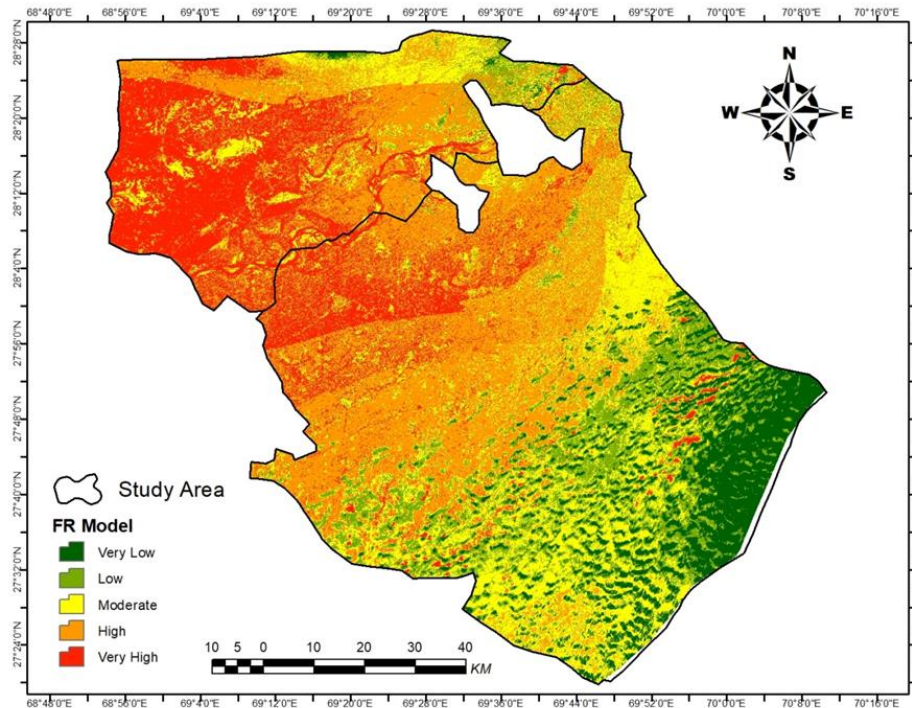


Figure 6: Flood Susceptibility Map of the Study Area Using Frequency Ratio Model

4. Validation through the Area under Curve (AUC)

A major result of the model is the flood forecast rate which is essential for checking how successful risk and susceptibility mapping is Tehrani et al. (2015). To prove the model, this work uses Area Under the Curve (AUC) while checking how well the positive findings correlated with negative ones (Fig. 6). A percentage of 30 of all flood points were selected and Equation(6) was used to assess the AUC value. According to the model, 75% of the tests were successful, as indicated by the AUC of 0.754. Satisfaction with this percentage was achieved despite the intrinsic limits of the data and how precise it was. It demonstrates how well the frequency ratio model and other variables predict flooding and measure how easy it is for floods to affect the study area.

5. Conclusion

Making maps of flood vulnerability is important for creating practical plans for flood disasters. Flood susceptibility data lets communities plan land use without any risk of flooding and assists planners by giving them useful knowledge. Researchers developed a flooding risk assessment visualization of both the urban centers of Rawalpindi and Islamabad utilizing a satellite imagery and GIS methodology in conjunction with a Biophysical Suitability Analysis (BSA) FR framework. A total of ten environmental parameters were examined: soil, LULC, rainfall, aspect, slope, elevation, road distance, river distance, NDVI and NDSI. At a 30-meter resolution, the inundation potential chart was utilized to create data layers and 130 samples were randomly selected, with 40 used for validation and the others for training. The precision with which each parameter layer is constructed is significant in determining flood-vulnerable area identification. The inundation probability was categorized into five classifications for the research region: minimal, slight, intermediate, severe and critical. Analysis demonstrated that 18.3, 30.9, 20.7, 20.6 and 9.31% of the terrain is extremely susceptible, highly susceptible, moderately, minimally and least likely to experience flooding. The area exhibits variation in flood susceptibility, starting with areas that are only moderately susceptible and ending with areas very susceptible to floods. It is mainly present in the central Ghotki area, covering Kacha, some mid-level areas in the district and by the Indus which have all been identified as being at high to very high risk. The western part of Kashmore district is particularly affected by the threat of floods. They are important parts of determining risk of flooding. When you look at the susceptibility assessments, you can expect "high" or "very

high" chances of future flooding. Evaluation using the ROC curve underscored the Frequency Ratio model's importance in vulnerability mapping, achieving a robust performance rate of 75%, indicating consistent and reliable results. Thus, it is concluded that model accuracy correlates positively with the quality of conditioning factors, emphasizing their pivotal role in flood susceptibility mapping. For Ghotki and Kashmore Districts' flood-prone zones, key factors influencing susceptibility include soil type (32.5), elevation (14.9), LULC (10.2), and rainfall (8.0). Understanding the patterns of extreme climatic events, particularly floods, and implementing recommended adaptation strategies are essential. By delineating flood-prone areas, this model assists policymakers, government representatives, planners, and decision-makers in creating suitable administrative plans and directing sustainable development strategies in the research area.

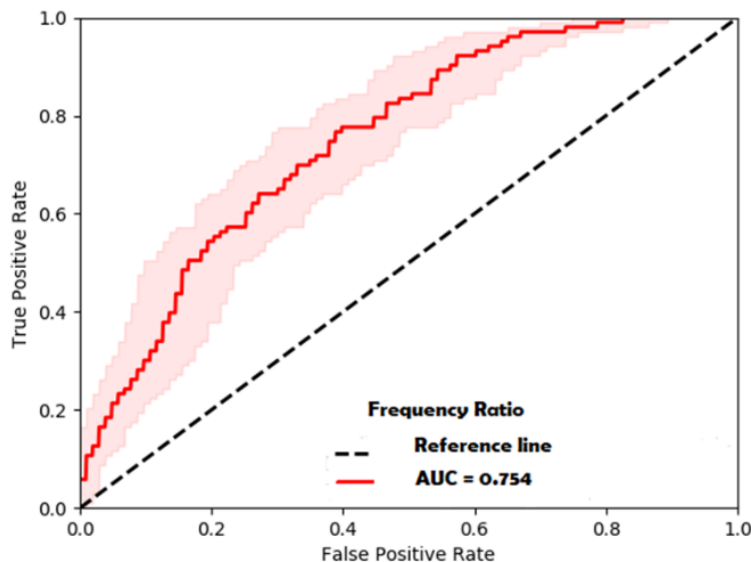


Figure 7: Showing Area Under the Curve (AUC) Validation Graph

Authors Contribution

Awais Munir: conceptualization, data analysis, and prepared the initial manuscript draft
 Muhammad Bachal Alias Sahib Khan: data interpretation and map generation
 Muhammad Asad Ghufuran: methodology design and supervised field data collection
 Noor Fatima: critical revision, incorporation of intellectual content and final editing
 All authors read and approved the final manuscript.

Conflict of Interests/Disclosures

The authors declared no potential conflicts of interest w.r.t. the research, authorship and/or publication of this article.

References

- Abd El-Hamid, H. T., Kaloop, M. R., Abdalla, E. M., Hu, J. W., & Zarzoura, F. (2021). Assessment and prediction of land-use/land-cover change around Blue Nile and White Nile due to flood hazards in Khartoum, Sudan, based on geospatial analysis. *Geomatics, Natural Hazards and Risk*, 12(1), 1258-1286. <https://doi.org/10.1080/19475705.2021.1923577>
- Aghdam, I. N., Varzandeh, M. H. M., & Pradhan, B. (2016). Landslide susceptibility mapping using an ensemble statistical index (Wi) and adaptive neuro-fuzzy inference system (ANFIS) model at Alborz Mountains (Iran). *Environmental Earth Sciences*, 75, 1-20.
- Alexander, K., Hettiarachchi, S., Ou, Y., & Sharma, A. (2019). Can integrated green spaces and storage facilities absorb the increased risk of flooding due to climate change in developed urban environments? *Journal of Hydrology*, 579, 124201. <https://doi.org/10.1016/j.jhydrol.2019.124201>
- Buba, F. N., Ojinnaka, O. C., Ndukwu, R. I., Agbaje, G. I., & Orofin, Z. O. (2021). Assessment of flood vulnerability in some communities in Lokoja, Kogi State, Nigeria, using

- Participatory Geographic Information Systems. *International Journal of Disaster Risk Reduction*, 55, 102111. <https://doi.org/10.1016/j.ijdrr.2021.102111>
- Bui, D. T., Ngo, P.-T. T., Pham, T. D., Jaafari, A., Minh, N. Q., Hoa, P. V., & Samui, P. (2019). A novel hybrid approach based on a swarm intelligence optimized extreme learning machine for flash flood susceptibility mapping. *CATENA*, 179, 184-196. <https://doi.org/10.1016/j.catena.2019.04.009>
- Chapi, K., Singh, V. P., Shirzadi, A., Shahabi, H., Bui, D. T., Pham, B. T., & Khosravi, K. (2017). A novel hybrid artificial intelligence approach for flood susceptibility assessment. *Environmental Modelling & Software*, 95, 229-245. <https://doi.org/10.1016/j.envsoft.2017.06.012>
- Chen, D., Wei, W., & Chen, L. (2020). How can terracing impact on soil moisture variation in China? A meta-analysis. *Agricultural Water Management*, 227, 105849. <https://doi.org/https://doi.org/10.1016/j.agwat.2019.105849>
- Choudhury, K. N., Yabar, H., & Mizunoya, T. (2022). GIS and remote sensing-based spatiotemporal analysis of cumulative flood risk over Bangladesh's national highways. *Asia-Pacific Journal of Regional Science*, 6(1), 335-364. <https://doi.org/10.1007/s41685-021-00216-5>
- Chung, C.-J. F., & Fabbri, A. G. (2003). Validation of Spatial Prediction Models for Landslide Hazard Mapping. *Natural Hazards*, 30(3), 451-472. <https://doi.org/10.1023/B:NHAZ.0000007172.62651.2b>
- Costache, R., & Tien Bui, D. (2020). Identification of areas prone to flash-flood phenomena using multiple-criteria decision-making, bivariate statistics, machine learning and their ensembles. *Science of The Total Environment*, 712, 136492. <https://doi.org/10.1016/j.scitotenv.2019.136492>
- Das, S. (2020). Flood susceptibility mapping of the Western Ghat coastal belt using multi-source geospatial data and analytical hierarchy process (AHP). *Remote Sensing Applications: Society and Environment*, 20, 100379. <https://doi.org/10.1016/j.rsase.2020.100379>
- Dodangeh, E., Singh, V. P., Pham, B. T., Yin, J., Yang, G., & Mosavi, A. (2020). Flood Frequency Analysis of Interconnected Rivers by Copulas. *Water Resources Management*, 34(11), 3533-3549. <https://doi.org/10.1007/s11269-020-02634-0>
- Gupta, K. (2020). Challenges in developing urban flood resilience in India. *Philosophical Transactions of the Royal Society A*, 378(2168), 20190211. <https://doi.org/https://doi.org/10.1098/rsta.2019.0211>
- Islam, A. R. M. T., Talukdar, S., Mahato, S., Kundu, S., Eibek, K. U., Pham, Q. B., . . . Linh, N. T. T. (2021). Flood susceptibility modelling using advanced ensemble machine learning models. *Geoscience Frontiers*, 12(3), 101075. <https://doi.org/https://doi.org/10.1016/j.gsf.2020.09.006>
- Khosravi, K., Nohani, E., Maroufinia, E., & Pourghasemi, H. R. (2016). A GIS-based flood susceptibility assessment and its mapping in Iran: a comparison between frequency ratio and weights-of-evidence bivariate statistical models with multi-criteria decision-making technique. *Natural Hazards*, 83(2), 947-987. <https://doi.org/10.1007/s11069-016-2357-2>
- Lee, M.-J., Kang, J.-e., & Jeon, S. (2012). Application of frequency ratio model and validation for predictive flooded area susceptibility mapping using GIS. 2012 IEEE international geoscience and remote sensing symposium, Germany.
- Liao, X., & Carin, L. (2009). Migratory logistic regression for learning concept drift between two data sets with application to UXO sensing. *IEEE Transactions on Geoscience and Remote Sensing*, 47(5), 1454-1466. <https://doi.org/https://doi.org/10.1109/TGRS.2008.2005268>
- Lu, W., Lei, H., Yang, W., Yang, J., & Yang, D. (2020). Comparison of Floods Driven by Tropical Cyclones and Monsoons in the Southeastern Coastal Region of China. *Journal of Hydrometeorology*, 21(7), 1589-1603. <https://doi.org/10.1175/JHM-D-20-0002.1>
- Mashaly, J., & Ghoneim, E. (2018). Flash Flood Hazard Using Optical, Radar, and Stereo-Pair Derived DEM: Eastern Desert, Egypt. *Remote Sensing*, 10(8), 1204. <https://doi.org/10.3390/rs10081204>
- Mehravar, S., Razavi-Termeh, S. V., Moghimi, A., Ranjgar, B., Foroughnia, F., & Amani, M. (2023). Flood susceptibility mapping using multi-temporal SAR imagery and novel

- integration of nature-inspired algorithms into support vector regression. *Journal of Hydrology*, 617, 129100. <https://doi.org/10.1016/j.jhydrol.2023.129100>
- Mitra, R., & Das, J. (2022). A comparative assessment of flood susceptibility modelling of GIS-based TOPSIS, VIKOR, and EDAS techniques in the Sub-Himalayan foothills region of Eastern India. *Environmental Science and Pollution Research*, 30(6), 16036-16067. <https://doi.org/10.1007/s11356-022-23168-5>
- Munir, A., Ghufuran, M., Ali, S., Majeed, A., Batool, A., Khan, M., & Abbasi, G. (2022). Flood Susceptibility Assessment Using FrequencyRatio Modelling Approach in Northern Sindhand Southern Punjab, Pakistan. *Polish Journal of Environmental Studies*, 31(4), 3249-3261. <https://doi.org/10.15244/pjoes/145607>
- Paul, G. C., Saha, S., & Hembram, T. K. (2019). Application of the GIS-Based Probabilistic Models for Mapping the Flood Susceptibility in Bansloi Sub-basin of Ganga-Bhagirathi River and Their Comparison. *Remote Sensing in Earth Systems Sciences*, 2(2-3), 120-146. <https://doi.org/10.1007/s41976-019-00018-6>
- Peptenatu, D., Grecu, A., Simion, A. G., Gruia, K. A., Andronache, I., Draghici, C. C., & Diaconu, D. C. (2020). Deforestation and Frequency of Floods in Romania. In A. M. Negm, G. Romanescu, & M. Zeleňáková (Eds.), *Water Resources Management in Romania* (pp. 279-306). Springer International Publishing.
- Philip, S., Sparrow, S., Kew, S. F., Van Der Wiel, K., Wanders, N., Singh, R., . . . Van Oldenborgh, G. J. (2019). Attributing the 2017 Bangladesh floods from meteorological and hydrological perspectives. *Hydrology and Earth System Sciences*, 23(3), 1409-1429. <https://doi.org/10.5194/hess-23-1409-2019>
- Pourghasemi, H. R., Amiri, M., Edalat, M., Ahrari, A. H., Panahi, M., Sadhasivam, N., & Lee, S. (2021). Assessment of Urban Infrastructures Exposed to Flood Using Susceptibility Map and Google Earth Engine. *IEEE Journal of Selected Topics in Applied Earth Observations and Remote Sensing*, 14, 1923-1937. <https://doi.org/10.1109/JSTARS.2020.3045278>
- Pourghasemi, H. R., Moradi, H. R., & Fatemi Aghda, S. M. (2013). Landslide susceptibility mapping by binary logistic regression, analytical hierarchy process, and statistical index models and assessment of their performances. *Natural Hazards*, 69(1), 749-779. <https://doi.org/10.1007/s11069-013-0728-5>
- Pradhan, B., & Buchroithner, M. F. (2010). Comparison and Validation of Landslide Susceptibility Maps Using an Artificial Neural Network Model for Three Test Areas in Malaysia. *Environmental and Engineering Geoscience*, 16(2), 107-126. <https://doi.org/10.2113/qseegeosci.16.2.107>
- Qamer, F. M., Ahmad, B., Hussain, A., Salman, A., Muhammad, S., Nawaz, M., . . . Thapa, S. (2022). *The 2022 Pakistan floods: Assessment of crop losses in Sindh Province using satellite data*.
- Rahman, M., Ningsheng, C., Mahmud, G. I., Islam, M. M., Pourghasemi, H. R., Ahmad, H., . . . Dewan, A. (2021). Flooding and its relationship with land cover change, population growth, and road density. *Geoscience Frontiers*, 12(6), 101224. <https://doi.org/10.1016/j.gsf.2021.101224>
- Rahmati, O., Pourghasemi, H. R., & Zeinivand, H. (2016). Flood susceptibility mapping using frequency ratio and weights-of-evidence models in the Golastan Province, Iran. *Geocarto International*, 31(1), 42-70. <https://doi.org/10.1080/10106049.2015.1041559>
- Regmi, A. D., Devkota, K. C., Yoshida, K., Pradhan, B., Pourghasemi, H. R., Kumamoto, T., & Akgun, A. (2014). Application of frequency ratio, statistical index, and weights-of-evidence models and their comparison in landslide susceptibility mapping in Central Nepal Himalaya. *Arabian Journal of Geosciences*, 7(2), 725-742. <https://doi.org/10.1007/s12517-012-0807-z>
- Shuster, W. D., Bonta, J., Thurston, H., Warnemuende, E., & Smith, D. R. (2005). Impacts of impervious surface on watershed hydrology: A review. *Urban Water Journal*, 2(4), 263-275. <https://doi.org/https://doi.org/10.1080/15730620500386529>
- Siswanto, S. Y., & Francés, F. (2019). How land use/land cover changes can affect water, flooding and sedimentation in a tropical watershed: a case study using distributed modeling in the Upper Citarum watershed, Indonesia. *Environmental Earth Sciences*, 78(17), 550. <https://doi.org/10.1007/s12665-019-8561-0>

- Sturzenegger, M., Holm, K., Lau, C.-A., & Jakob, M. (2019). Semi-automated regional scale debris-flow and debris-flood susceptibility mapping based on digital elevation model metrics and Flow-R software.
- Tehrany, M. S., Pradhan, B., & Jebur, M. N. (2015). Flood susceptibility analysis and its verification using a novel ensemble support vector machine and frequency ratio method. *Stochastic Environmental Research and Risk Assessment*, 29(4), 1149-1165. <https://doi.org/10.1007/s00477-015-1021-9>
- Van Binh, D., Kantoush, S. A., Saber, M., Mai, N. P., Maskey, S., Phong, D. T., & Sumi, T. (2020). Long-term alterations of flow regimes of the Mekong River and adaptation strategies for the Vietnamese Mekong Delta. *Journal of Hydrology: Regional Studies*, 32, 100742. <https://doi.org/https://doi.org/10.1016/j.ejrh.2020.100742>
- Wang, Y., Hong, H., Chen, W., Li, S., Pamučar, D., Gigović, L., . . . Duan, H. (2018). A Hybrid GIS Multi-Criteria Decision-Making Method for Flood Susceptibility Mapping at Shangyou, China. *Remote Sensing*, 11(1), 62. <https://doi.org/10.3390/rs11010062>
- Yesilnacar, E., & Hunter, G. J. (2004). Application of Neural Networks for Landslide Susceptibility Mapping in Turkey. In J. P. Van Leeuwen & H. J. P. Timmermans (Eds.), *Recent Advances in Design and Decision Support Systems in Architecture and Urban Planning* (pp. 3-18). Springer Netherlands.
- Zhao, Y., Cao, W., Hu, C., Wang, Y., Wang, Z., Zhang, X., . . . Xie, G. (2019). Analysis of changes in characteristics of flood and sediment yield in typical basins of the Yellow River under extreme rainfall events. *CATENA*, 177, 31-40. <https://doi.org/10.1016/j.catena.2019.02.001>
- Zou, Q., Zhou, J., Zhou, C., Song, L., & Guo, J. (2013). Comprehensive flood risk assessment based on set pair analysis-variable fuzzy sets model and fuzzy AHP. *Stochastic Environmental Research and Risk Assessment*, 27, 525-546. <https://doi.org/https://doi.org/10.1007/s00477-012-0598-5>